

Pressure influence on bound polarons in a strained wurtzite GaN/Al_xGa_{1-x}N heterojunction under an electric field*

Zhang Min(张敏)^{1,2} and Ban Shiliang(班士良)^{1,†}

(1 Department of Physics, School of Physical Science and Technology, Inner Mongolia University, Hohhot 010021, China)

(2 College of Physics and Electron Information, Inner Mongolia Normal University, Hohhot 010022, China)

Abstract: The binding energies of bound polarons near the interface of a strained wurtzite GaN/Al_xGa_{1-x}N heterojunction are studied by using a modified LLP variational method and a simplified coherent potential approximation under hydrostatic pressure and an external electric field. Considering the biaxial strain due to lattice mismatch or epitaxial growth, the uniaxial strain effects and the influences of the electron–phonon interaction as well as impurity–phonon interaction including the effects of interface–optical phonon modes and half-space phonon modes, the binding energies as functions of pressure, the impurity position, areal electron density and the phonon effect on the Stark energy shift are investigated. The numerical result shows that the contributions from the interface optical phonon mode with higher frequency and the LO-like half space mode to the binding energy and the Stark energy shift are important and obviously increase with increasing hydrostatic pressure, whereas the interface optical phonon mode with lower frequency and the TO-like half space mode are extremely small and are insensitive to the impurity position and hydrostatic pressure. It is also shown that the conductive band bending should not be neglected.

Key words: bound polaron; strained wurtzite heterojunction; pressure; electric field

DOI: 10.1088/1674-4926/31/5/052002

PACC: 6320K; 7138; 7155G

1. Introduction

In recent years, hexagonal wurtzite nitride semiconductors of group-III with wide-band-gaps and related compounds materials have found important applications in high-power, high-frequency electronic devices because of their fascinating properties. Compared to zinc-blende structure, wurtzite crystals have a different unit-cell as well as lower symmetry resulting in some abnormal properties such as optical phonons. There are many distinct phonon branches (nine optical modes and three acoustic modes) associated with the wurtzite nitride polar crystals. At the same time, the phonon modes may be neither purely longitudinal nor transverse except for the [0001] direction. The lattice vibration can be divided into two groups of phonons: ordinary and extraordinary. Two of the extraordinary optical branches corresponding to the A₁ and E₁ are Roman and infrared active. Furthermore, the A₁ and E₁ modes split into longitudinally optical (LO) and transversely optical (TO) components. As a result, the phonon dynamics and electron–phonon interaction in this kind of materials may be substantially different from those with cubic symmetry. In particular, the strain effect also plays an important role since the electronic and optical properties of semiconductor heterostructures depend crucially on the strain due to the lattice mismatch between the two sublayers. Previously, Jogai studied the effect of strain on wurtzite GaN by using a tight-binding model^[1]. Recently, Shi calculated the interface optical-phonon modes in strained wurtzite GaN/AlN quantum wells^[2]. More recently, Pokatilov *et al.* studied theoretically the exciton states and pho-

toluminescence spectra of strained wurtzite Al_xGa_{1-x}N/GaN quantum-well heterostructures^[3].

High pressure technology has also become an important tool in determining the band structures and understanding the electronic and optical properties of materials. As a result, the optical properties of wurtzite InGaN/GaN and GaN/AlGaN QWs under hydrostatic pressure have been extensively studied^[4–6]. Goñi *et al.* investigated the pressure modification on phonon modes in hexagonal (wurtzite) and cubic (zinc-blende) GaN and hexagonal AlN, respectively^[7]. Ha *et al.* presented the binding energies of excitons in a strained wurtzite GaN/AlGaN quantum well by considering the hydrostatic pressure effect and screening due to the electron–hole gas^[8].

The bound polarons in semiconductor heterostructures have been an interesting subject both in theory and experiment since they present novel photoelectric properties different from those in bulk materials. We have studied the properties of bound polarons under an external magnetic field and hydrostatic pressure^[9] focusing on the zinc-blend structure. Due to the lower symmetry of the unit-cell structure in the wurtzite materials, some authors investigated the optical phonon modes and electron–optical phonon interaction in the structure^[10–12]. However, most of the works concentrated on the electron–phonon interaction in quantum wells or heterojunctions but did not include the interactions of the impurity with phonons and the influence from the real potential barrier near the interface.

In this article, we investigate the bound polaron properties including the pressure and electric field effects on strained

* Project supported by the National Natural Science Foundation of China (No. 60966001), the Key Project of Natural Science Foundation of Inner Mongolia Autonomous Region, China (No. 20080404Zd02), and the Specialized Research Fund for the Doctoral Program of Higher Education of China (No. 20070126001).

† Corresponding author. Email: slban@imu.edu.cn

Received 24 November 2009, revised manuscript received 16 January 2010

© 2010 Chinese Institute of Electronics

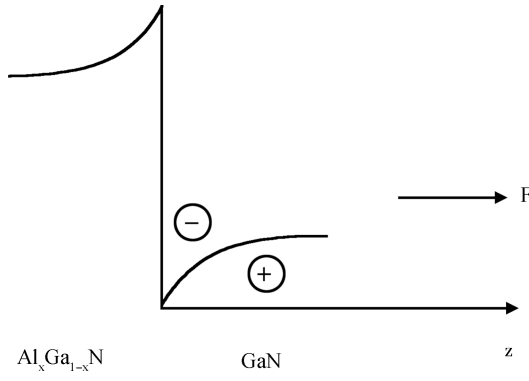


Fig. 1. A schematic diagram of a heterojunction consisting of a channel side GaN and a barrier side GaN/Al_xGa_{1-x}N with an electric field in the z-direction. The solid curve indicates the band potential acting on an electron denoted by “-” and “+” indicates an impurity.

(0001)-oriented wurtzite structures. A modified LLP variational method and a simplified coherent potential approximation (SCPA) have been adopted to treat some transform formulae and parameters. The interaction between an impurity and the interface-optical (IF) phonon modes and half-space (HS) phonon modes in a strained wurtzite heterojunction is considered. We also show the numerical results for the relations between the binding energies, impurity position and electric areal density.

2. Model and calculation

Let us now consider a free strained wurtzite GaN/Al_x-Ga_{1-x}N heterojunction whose channel side GaN, denoted by material 1, is located at $z > 0$ and barrier side Al_xGa_{1-x}N, denoted by material 2, is located at $z < 0$, respectively (see Fig. 1). The interface of the heterojunction is defined as the x - y plane, which is assumed infinite without losing generality. By considering the interaction from the IF and HS phonons, the Hamiltonian of the system consisting of an electron with charge $-e$ affected by a hydrogen-like impurity and optical phonons in an external electric field F along the z -direction can be written as

$$H = H_e + H_c + H_{ph} + H_{e,i-ph}, \quad (1)$$

where

$$H_e = \left(\frac{p_{\perp}^2}{2m_{\perp\lambda}} + \frac{p_z^2}{2m_{z\lambda}} \right) \theta(\lambda, z) + V(z) + eFz, \quad \lambda = 1, 2, \quad (2)$$

$$H_c = -\frac{e^2}{\kappa_{\infty}(z, z_0)[x^2 + y^2 + (z - z_0)^2]^{1/2}}. \quad (3)$$

The symbols used in Eqs. (2) and (3) have been defined in previous work^[13] except for the electron (impurity)-phonon interaction as well as the optical dielectric constant $\kappa_{\infty}(z, z_0)$ instead of a static one. The third term in Eq. (1) is the Hamiltonian for a free phonon field which has the well-known form

$$H_{ph} = \sum_{\mathbf{k}, \lambda} \hbar \omega_{HS} a_{\mathbf{k}\lambda}^{\dagger} a_{\mathbf{k}\lambda} \theta(\lambda, z) + \sum_{\mathbf{q}, \sigma} \hbar \omega_{IF} b_{\mathbf{q}\sigma}^{\dagger} b_{\mathbf{q}\sigma}, \quad (4)$$

where $a_{\mathbf{k}\lambda}^{\dagger}$ ($a_{\mathbf{k}\lambda}$) is the creation (annihilation) operator of an HS phonon with wave vector \mathbf{k} and frequency ω_{HS} in the λ

material, and $b_{\mathbf{q}\sigma}^{\dagger}$ ($b_{\mathbf{q}\sigma}$) is the counterpart of an IF phonon with wave vector \mathbf{q} and frequency ω_{IF} .

The fourth term in Eq. (1) is the electron (impurity)-phonon interaction term and can be written as

$$H_{e,i-ph} = H_{e,i-HS} + H_{e,i-IF}, \quad (5)$$

where $H_{e,i-HS}$ and $H_{e,i-IF}$ stand for the Hamiltonians of the interactions between the electron and the HS and the IF phonons, respectively. It can be given as follows.

$$H_{e,i-HS} = \sum_{\mathbf{k}_{\perp}} \sum_{k_{1z} > 0} (A_{\mathbf{k}} M_{\mathbf{k}} a_{\mathbf{k}_{\perp}\lambda} + h.c.), \quad (6)$$

where

$$A_{\mathbf{k}} = \left[\frac{4\pi e^2 \hbar L^{-3}}{(\partial/\partial\omega)(\kappa_{1\perp} \sin^2 \theta_1 + \kappa_{1z} \cos^2 \theta_1)} \right]^{1/2} \times \frac{1}{\sqrt{k_{\perp}^2 + k_{1z}^2}} \frac{2}{\sqrt{\kappa_{1z}^2 k_{1z}^2 + \kappa_{2z} \kappa_{2\perp} k_{\perp}^2}}, \quad (7)$$

and

$$M_{\mathbf{k}} = \begin{cases} \kappa_{1z} k_{1z} [\cos(k_{1z} z) e^{i\mathbf{k}_{\perp} \cdot \boldsymbol{\rho}} - \cos(k_{1z} z_0)] + \\ \sqrt{\kappa_{2z} \kappa_{2\perp}} k_{\perp} [\sin(k_{1z} z) e^{i\mathbf{k}_{\perp} \cdot \boldsymbol{\rho}} - \sin(k_{1z} z_0)], & z > 0, \\ \kappa_{1z} k_{1z} e^{i\mathbf{k}_{\perp} \cdot \boldsymbol{\rho}} e^{\sqrt{\kappa_{2\perp}/\kappa_{2z}} k_{\perp} (z - z_0)}, & z < 0. \end{cases} \quad (8)$$

The Hamiltonian for the counterpart of IF phonons is written as

$$H_{e,i-IF} = \sum_{\mathbf{q}, \sigma} \left[\frac{B_{\sigma}}{\sqrt{q}} \left(e^{-i\mathbf{q} \cdot \boldsymbol{\rho}} e^{-\sqrt{\kappa_{\lambda\perp}/\kappa_{\lambda z}} q|z|} - e^{-\sqrt{\kappa_{\lambda\perp}/\kappa_{\lambda z}} q|z_0|} \right) b_{\mathbf{q}\sigma} + h.c \right], \quad (9)$$

$$B_{\sigma} = \left[\frac{4\pi e^2 \hbar L^{-2}}{[(\partial/\partial\omega)(\sqrt{\kappa_{1\perp} \kappa_{1z}} - \sqrt{\kappa_{2\perp} \kappa_{2z}})]} \right]^{1/2}. \quad (10)$$

The IF modes can exist if solutions can be found for the dispersion relation $\sqrt{\kappa_{1\perp} \kappa_{1z}} - \sqrt{\kappa_{2\perp} \kappa_{2z}} = 0$ with $\kappa_{1\perp} \kappa_{1z} > 0$, $\kappa_{2\perp} \kappa_{2z} > 0$, and $\kappa_{1\perp} \kappa_{2z} < 0$ ^[9].

The direction-dependent dielectric functions, $\kappa_{\perp}(\omega)$ and $\kappa_z(\omega)$, are given by

$$\kappa_{\perp}(\omega) = \kappa_{\perp}^{\infty} \frac{\omega^2 - \omega_{\perp L}^2}{\omega^2 - \omega_{\perp T}^2}, \quad (11)$$

$$\kappa_z(\omega) = \kappa_z^{\infty} \frac{\omega^2 - \omega_{z L}^2}{\omega^2 - \omega_{z T}^2}, \quad (12)$$

where $\omega_{\perp L}$ and $\omega_{z L}$ are the frequencies of LO phonons and $\omega_{\perp T}$ and $\omega_{z T}$ are those of TO phonons. κ_{\perp}^{∞} and κ_z^{∞} are high-frequency dielectric constants.

The frequencies for extraordinary phonons are obtained from

$$\kappa_{\perp}(\omega) \sin^2 \theta + \kappa_z(\omega) \cos^2 \theta = 0. \quad (13)$$

When $|\omega_{\perp L} - \omega_{z L}|$, $|\omega_{\perp T} - \omega_{z T}| \ll |\omega_{\perp L} - \omega_{z T}|$, $|\omega_{z L} - \omega_{z T}|$ for wurtzite-based nitrides materials, the solutions become

$$\omega_L^2 = \omega_{z L}^2 \cos^2 \theta + \omega_{\perp L}^2 \sin^2 \theta, \quad (14)$$

$$\omega_T^2 = \omega_{z T}^2 \sin^2 \theta + \omega_{\perp T}^2 \cos^2 \theta. \quad (15)$$

Equations (14) and (15) presents the characteristic frequencies of predominantly LO-like and TO-like modes, respectively.

We extend the LLP method to the present situation where the electron couples with the branches of the HS phonon modes and the IF optical phonon modes with two unitary transformations as follows:

$$U_1 = \exp \left[\frac{-i}{\hbar} \left(\hbar \sum_{\mathbf{k}, \lambda} \mathbf{k} a_{\mathbf{k}\lambda}^+ a_{\mathbf{k}\lambda} \theta(\lambda, z) + \hbar \sum_{\mathbf{q}, \sigma} \mathbf{q} b_{\mathbf{q}\sigma}^+ b_{\mathbf{q}\sigma} \right) \cdot \boldsymbol{\rho} \right], \quad (16)$$

$$U_2 = \exp \left[\sum_{\mathbf{k}, \lambda} (f_{\mathbf{k}\lambda} a_{\mathbf{k}\lambda}^+ - f_{\mathbf{k}\lambda}^* a_{\mathbf{k}\lambda}) \theta(\lambda, z) + \sum_{\mathbf{q}, \sigma} (g_{\mathbf{q}\sigma} b_{\mathbf{q}\sigma}^+ - g_{\mathbf{q}\sigma}^* b_{\mathbf{q}\sigma}) \right], \quad (17)$$

in which $f_{\mathbf{k}}$, $g_{\mathbf{q}\sigma}$ and their complex conjugates are variational parameters.

The wave function of an electron in a triangle-like potential is usually solved by a complex Airy function, but we here adopt a simple trial wave function, which can be chosen as^[13]

$$\psi(x, y, z) = \varphi(x, y) \xi(z) = \varphi(\boldsymbol{\rho}) \xi(z) \prod_{\mathbf{k}, \lambda, \mathbf{q}, \sigma} |0_{\mathbf{k}\lambda}\rangle |0_{\mathbf{q}, \sigma}\rangle, \quad (18)$$

where

$$\varphi(\boldsymbol{\rho}) = \left[\frac{1}{2\pi} \right]^{1/2} \gamma e^{i\mathbf{k} \cdot \boldsymbol{\rho}} e^{-\gamma \rho / 2}, \quad (19)$$

$$\xi(z) = \begin{cases} \xi_1(z) = B b^{1/2} (bz + \beta) e^{-bz/2}, & z > 0 \\ \xi_2(z) = D d^{1/2} e^{dz/2}, & z < 0 \end{cases} \quad (20)$$

In the above equation, b , d are variational parameters, and the normalization constants satisfy $\beta = 2b/(b + d)$, $B = [\beta^2(1 + b/d) + 2\beta + 2]^{-1/2}$ and $D = B\beta(b/d)^{1/2}$.

Thus, the variational energy of the bound polaron at ground state can be obtained as

$$E_{\text{bp}}(b, d) = \langle \psi | U_2^{-1} U_1^{-1} H U_1 U_2 | \psi \rangle = E_e + E_c - E_{\text{HS}} - E_{\text{IF}}, \quad (21)$$

where

$$E_{\text{HS}} = \sum_{\mathbf{k}} \frac{|\langle \psi | A_{\mathbf{k}} M_{\mathbf{k}} e^{-i\mathbf{k} \cdot \boldsymbol{\rho}} | \psi \rangle|^2}{\hbar \omega_{\text{HS}} + \frac{\hbar^2 k^2}{2m}}, \quad (22)$$

and

$$E_{\text{IF}} = \sum_{\mathbf{q}, \sigma} \left| \langle \psi | \frac{B_{\sigma}}{\sqrt{q}} \left(e^{-\sqrt{\kappa_{\lambda\perp}/\kappa_{\lambda z} q} |z|} - e^{-\sqrt{\kappa_{\lambda\perp}/\kappa_{\lambda z} q} |z_0|} \right) \times e^{-i\mathbf{q} \cdot \boldsymbol{\rho}} | \psi \rangle \right|^2 (\hbar \omega_{\text{IF}} + \frac{\hbar^2 q^2}{2m})^{-1}. \quad (23)$$

If we ignore H_c in Eq. (1), remove z_0 from Eqs. (8) and (9), and replace Eq. (19) by $\varphi(\boldsymbol{\rho}) = e^{i\mathbf{k} \cdot \boldsymbol{\rho}} / \sqrt{2\pi\hbar}$, the ground state energy E_{fp} for a free polaron can also be derived by using the

same process. Then, the binding energy of the bound polaron at ground state can be written as

$$E_{\text{B}} = E_{\text{fp}} - E_{\text{bp}}. \quad (24)$$

3. Pressure and strain dependence of physical parameters

Under hydrostatic pressure P , the components of biaxial stress tensors are equal to $\varepsilon_{xx, i} = \varepsilon_{yy, i} = \varepsilon_{zz, i}$, and Hooke's law gives a relationship between the components of the uniaxial and biaxial strain tensor $\varepsilon_{zz, i} = R^H \varepsilon_{xx, i}$ ^[14] with coefficient

$$R^H = \frac{C_{11, i}(P) + C_{12, i}(P) - 2C_{13, i}(P)}{C_{33, i}(P) - C_{13, i}(P)}, \quad i = 1, 2, \quad (25)$$

where $C_{\alpha\beta, i}(P)$ is the pressure-dependent elastic constants for wurtzite nitrides and satisfies

$$C_{\alpha\beta, i}(P) = C_{\alpha\beta, i}(0) + \gamma_{\alpha\beta, i} P + \delta_{\alpha\beta, i} P^2. \quad (26)$$

In Eq. (26), coefficients $\gamma_{\alpha\beta, i}$ and $\delta_{\alpha\beta, i}$ were given in Ref. [15].

In a GaN/Al_xGa_{1-x}N real heterojunction, the biaxial lattice-mismatch-induced strain is given as

$$\begin{cases} \varepsilon_{xx, 1} = \varepsilon_{yy, 1} = \frac{a_2(P) - a_1(P)}{a_1(P)}, \\ \varepsilon_{xx, 2} = \varepsilon_{yy, 2} = \frac{a_1(P) - a_2(P)}{a_2(P)}, \end{cases} \quad (27)$$

where the lattice constant affected by hydrostatic pressure^[16] is

$$a_i(P) = a_i(0) \left(1 - \frac{P}{3B_{0, i}(P)} \right), \quad i = 1, 2. \quad (28)$$

The bulk modulus $B_{0, i}(P)$ in a wurtzite structure is related to the elastic constants by

$$B_{0, i}(P) = \frac{[C_{11, i}(P) + C_{12, i}(P)]C_{33, i}(P) - 2C_{13, i}^2(P)}{C_{11, i}(P) + C_{12, i}(P) + 2C_{33, i}(P) - 4C_{13, i}(P)}, \quad i = 1, 2. \quad (29)$$

For wurtzites GaN and AlN, the lowest conduction band and the top of the valence band are situated at the Γ point. Considering the effect of strain, hydrostatic pressure and negative crystal field splitting without spin-orbit interaction, the energy gaps of GaN and AlN are^[17]

$$E_{\text{g, GaN}}(P, \varepsilon) = E_{\text{g, GaN}}(P) + 2(a_{1, \text{GaN}} + b_{1, \text{GaN}})\varepsilon_{xx, \text{GaN}} + (a_{2, \text{GaN}} + b_{2, \text{GaN}})\varepsilon_{zz, \text{GaN}}, \quad (30)$$

and

$$E_{\text{g, AlN}}(P, \varepsilon) = E_{\text{g, AlN}}(P) + 2a_{1, \text{AlN}}\varepsilon_{xx, \text{AlN}} + a_{2, \text{AlN}}\varepsilon_{zz, \text{AlN}}, \quad (31)$$

where the pressure-dependent energy gaps are considered by the following expression^[18]

$$E_{\text{g, i}}(p) = E_{\text{g, i}}(0) + \alpha_i P + \beta_i P^2. \quad (32)$$

Table 1. Parameters used in the computations.

Material	a	E_g	α	β	C_{11}	C_{12}	C_{13}	C_{33}
GaN	3.189 ^a	3.507 ^a	39 ^b	-0.32 ^b	366 ^c	139 ^c	98 ^c	403 ^c
AlN	3.122 ^a	6.23 ^a	40 ^b	-0.32 ^b	397 ^c	143 ^c	112 ^c	372 ^c

^a Ref. [23], ^b Ref. [18], ^c Ref. [15].

Table 2. Parameters used in the computations.

Material	$\kappa_{\infty,xx}$	$\kappa_{\infty,zz}$	$\omega_{LO,xx}$	$\omega_{LO,zz}$	$\omega_{TO,xx}$	$\omega_{TO,zz}$	$\gamma_{LO,xx}$	$\gamma_{LO,zz}$	$\gamma_{TO,xx}$	$\gamma_{TO,zz}$
GaN	5.20 ^d	5.39 ^d	757 ^e	748 ^e	568 ^e	540 ^e	0.91 ^e	0.82 ^e	1.18 ^e	1.02 ^e
AlN	4.30 ^d	4.52 ^d	924 ^e	898 ^e	677 ^e	618 ^e	0.99 ^e	0.98 ^e	1.19 ^e	1.21 ^e

^d Ref. [14], ^e Ref. [24].

In Eqs.(30) and (31), $a_{1,i}$ and $a_{2,i}$ are the deformation potentials of the interband transition, $b_{1,i}$ and $b_{2,i}$ are the same potentials with crystal field splitting for a binary compound material i . Then, the energy gap of $\text{Al}_x\text{Ga}_{1-x}\text{N}$ can be calculated with the SCPA^[19]

$$E_{\text{TMC}} = \frac{E_A E_B}{x E_A + (1-x) E_B}. \quad (33)$$

Since the ratio of the conduction band to valence band offset is given to be 65 : 20 in a strained wurtzite nitride QW^[20], the barrier height V_0 can be determined by

$$V_0 = 0.765(E_{g,\text{GaN}} - E_{g,\text{AlGaN}}), \quad (34)$$

where $E_{g,\text{AlGaN}}$ and $E_{g,\text{GaN}}$ are the energy gaps of $\text{Al}_x\text{Ga}_{1-x}\text{N}$ and GaN, respectively.

The biaxial, uniaxial and hydrostatic pressure dependences of the effective mass^[21] of an electron in the z direction and x - y plane can be calculated by

$$\frac{m_{i,\alpha\alpha}^0}{m_{i,\alpha\alpha}(P)} = 1 + \frac{C_i}{E_{g,i}(P)}, \quad i = 1, 2, \quad \alpha = x, z, \quad (35)$$

where C_i is a fixed value for a given material with $P = 0$. The effective mass of an electron in $\text{Al}_x\text{Ga}_{1-x}\text{N}$ can be obtained by a linear interpolation method.

The frequencies of LO and TO phonons affected by strain can be written as^[14]

$$\omega_{j,\alpha\alpha} = \omega_{j,\alpha\alpha}(0) + 2K_{j, //} \varepsilon_{//} + K_{j, \perp} \varepsilon_{\perp}, \quad j = A_1, E_1, \quad (36)$$

where $K_{j, //}$ and $K_{j, \perp}$ are the strain coefficients related to the deformation potential of phonon modes.

Furthermore, the hydrostatic pressure dependence of $\omega_{j,\alpha\alpha}$ can be determined by the given mode-Grüneisen parameters

$$\gamma_{j,\alpha\alpha} = B_0 \frac{1}{\omega_{j,\alpha\alpha}} \frac{\partial \omega_{j,\alpha\alpha}(P)}{\partial P}. \quad (37)$$

The influence of hydrostatic pressure on the high frequency dielectric constants is given in Ref. [22], and can be written as

$$\frac{\partial \kappa_{\infty,\alpha\alpha}(p)}{\partial p} = -\frac{5(\kappa_{\infty,\alpha\alpha} - 1)}{3B_0} (0.9 - f_i), \quad (38)$$

where f_i is the ionicity of the material under pressure. Then the hydrostatic-pressure-modified biaxial and uniaxial strain dependence of the static dielectric constants is fully considered,

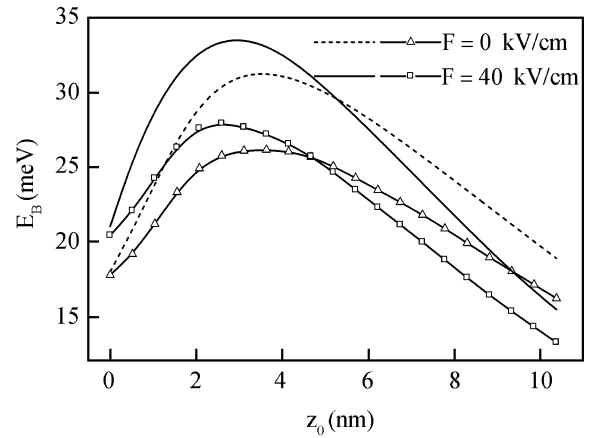


Fig. 2. Binding energies of polarons in a strained wurtzite GaN/ $\text{Al}_x\text{Ga}_{1-x}\text{N}$ heterojunction as functions of impurity position z_0 under zero and nonzero electric fields. The symbol curves and the bare curves are the results with and without the phonon effect, respectively.

whereas the dielectric constant of $\text{Al}_x\text{Ga}_{1-x}\text{N}$ can be calculated by the SCPA^[19]

$$\kappa_{\text{TMC}} = \left\{ [(1-x)m_B \kappa_A^2 + x m_A \kappa_B^2] (x/m_A + (1-x)/m_B) \right\}^{1/2}. \quad (39)$$

4. Numerical results and discussion

To understand the properties of the polarons in wurtzite nitride semiconductors, we performed numerical computation for a hexagonal GaN/ $\text{Al}_x\text{Ga}_{1-x}\text{N}$ heterojunction with biaxial and uniaxial free strain by considering the hydrostatic pressure effect with an external electric field. The calculated results are shown in Figs.1–6.

The parameters used in our computations are listed in Tables 1 and 2. For a free strained wurtzite GaN/ $\text{Al}_x\text{Ga}_{1-x}\text{N}$ heterojunction with [0001] orientation, the given Al concentration $x = 0.3$ and areal electronic density $n_s = 4.0 \times 10^{12} \text{ cm}^{-2}$, the relation between the polaronic binding energies E_B and the impurity position z_0 is given by Fig. 2. The results without phonon effect, which have been discussed in our previous paper for a wurtzite GaN/ $\text{Al}_x\text{Ga}_{1-x}\text{N}$ heterojunction^[25], are also plotted for comparison. One can clearly see that the negative contribution from optical phonons is important to decrease E_B for a larger z_0 , and the electric field F increases this decrease.

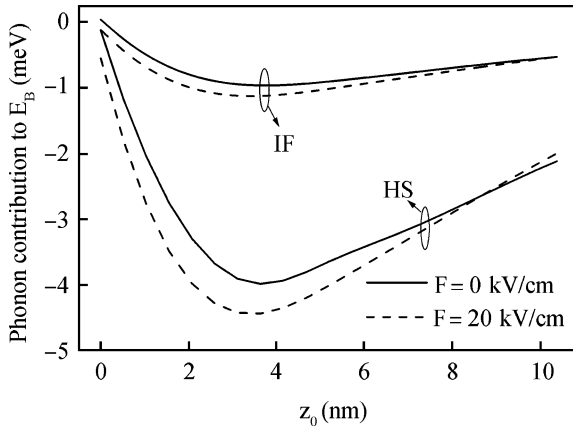


Fig. 3. Contributions to the binding energies from the IF and HS phonon modes as functions of impurity position z_0 under zero and nonzero electric fields at zero pressure.

As z_0 increases from zero the negative contribution increases from a small value and gradually reaches a maximum and then decreases slowly. Explanations for the maximum under zero field and nonzero field have been given in Refs. [13, 25], respectively. It should be pointed out that phonons enhance the F induced movement of the peak of E_B to the interface since the phonon effect decreases the Coulombic interaction between an impurity and an electron. Moreover, the negative contributions from phonons to E_B are respectively 16.4% and 16.8% for $F = 0$ and 40 kV/cm around the maxima since F enhances the Coulombic interaction and therefore weakens the polarization of a bound polaron for the average position \bar{z} of the electron being larger than z_0 .

Figure 3 shows the contributions to E_B from the HS and IF phonon modes as functions of z_0 at zero pressure. It can be seen that the HS phonons make a larger negative contribution to E_B than the IF phonons do and both of them increase to their maxima and then decrease gradually with z_0 departing from the interface. It can be also seen that F increases the contribution from the IF phonons since it overcomes the Coulombic attraction of the impurity and enforces the electron moving towards the interface for a small z_0 . Within a large region of $z_0 > 0$, F weakens the total polarization of the impurity–electron pair when $\bar{z} < z_0$, and the main polarization is from the impurity even when the polarization of the electron is enhanced. As a result, the negative contributions from phonons show a net increase, e.g. for $F = 20$ kV/cm, compared with that of zero electric field when $z_0 < 8.8$ nm. When $z_0 > 8.8$ nm, the main polarization is from the impurity but that from the electron is comparatively small since the HS phonons become dominant, to result in a cross of the two curves with and without F . A similar property can be seen from Fig. 2. Furthermore, our results also show that the contribution induced by the interactions between the pair and the LO-like phonons is approximately two orders larger than that induced by the TO-like phonons so that the latter can be neglected. It should be pointed out that the contribution from the IF phonon mode with a higher frequency is significant even when the HS mode plays an important role, whereas the mode with a lower frequency is extremely small, so that it can also be neglected in further work.

We plot in Fig. 4(a) the relation between E_B and hydro-

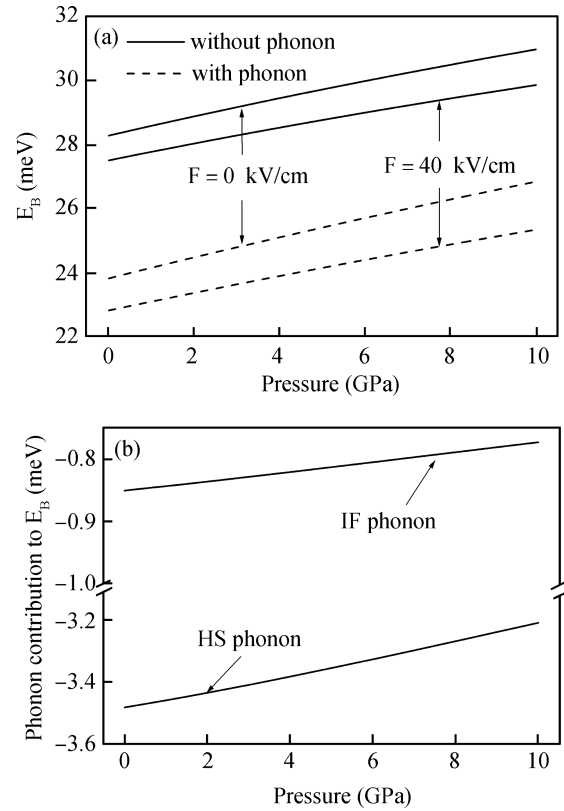


Fig. 4. (a) Binding energies and (b) contributions from the IF and HS phonon modes to the polaron in a free strained wurtzite GaN/Al_xGa_{1-x}N heterojunction with [0001] orientation as functions of hydrostatic pressure for impurity position $z_0 = 6$ nm.

static pressure P for electric fields $F = 0$ and 40 kV/cm for impurity position $z_0 = 6$ nm. A similar result to that for a zinc-blende heterojunction^[25] is obtained, to indicate that E_B increases nearly linearly with hydrostatic pressure. It can also be seen that the influence from phonons decreases E_B , since the pressure dependence of the physical parameters such as dielectric constant, phonon frequencies and the multi-effect influences the conduction band bending, electronic effective mass and barrier height. These factors cause the two-dimensional property of an electron to be more prominent and strengthen the phonon influence gradually as pressure increases. When pressure ranges from 0 to 10 GPa, the net increment of binding energies of bound polarons are 3.02 and 2.53 meV with percentages of 12.7% and 11.08% for $F = 0$ and 40 kV/cm by considering the effect of phonon modes. In the same circumstance without the phonon effect, the net increments of E_B are 2.695, 2.355 meV with percentages of 9.5% and 8.57%. This fact shows that E_B becomes more sensitive to the hydrostatic pressure P when the phonon effect is considered.

In order to see the contributions from the IF and HS phonons to E_B , their net contributions to E_B under zero electric field are illustrated in Fig. 4(b). One can clearly see that the characteristics of the two contributions have the same tendency with increasing hydrostatic pressure: that the HS phonon contribution decreases by 8.53% when pressure changes from 0 to 10 GPa whereas the IF phonon contribution decreases by 10.1% shows that the hydrostatic pressure effect is obvious and the rate of increase of IF phonons is larger than that of HS

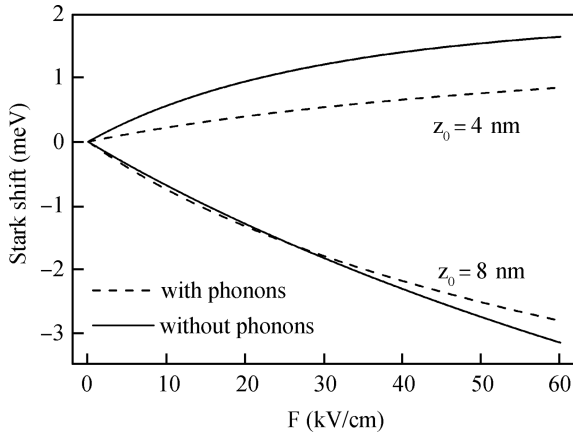


Fig. 5. Stark energy shift of polarons for different impurity positions as a function of the electric field.

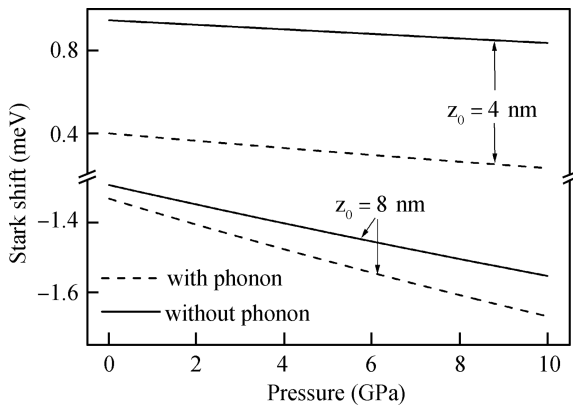


Fig. 6. Stark energy shift of polarons as a function of hydrostatic pressure for different impurity positions under an electric field $F = 20$ kV/cm.

phonons.

In Fig. 5, we display the Stark shift of a bound polaron as a function of the electric field for different impurity positions. For comparison, the Stark energy shift of the impurity state without phonons is also presented. A non-monotonous blue (red) shift of the Stark effect with increasing F can be clearly seen when the impurity is located at 4 and 8 nm. As discussed above (see Fig. 3), F weakens the total polarization of the impurity–electron pair when $\bar{z} < z_0$ for $z_0 = 4$ nm; the main polarization is from the impurity even when the polarization of the electron is enhanced. Considering the phonon effect, the blue shift significantly decreases, and the red shift increases slightly as $F < 28$ kV/cm but decreases as $F > 28$ kV/cm.

In Fig. 6, we perform the pressure influence on the Stark effect for impurity states and bound polarons with impurity position $z_0 = 4$ and 8 nm. It can be seen that P decreases the blue shift with $z_0 = 4$ nm, but increases the red shift with $z_0 = 8$ nm. The effect of hydrostatic pressure on the energy shift becomes more significant when the phononic effect is considered. When P ranges from 0 to 10 GPa, the Stark shift increases by 20.2% for a single impurity state whereas that with the phonon effect increases by 25.2% in comparison with that without phonons. This indicates that pressure and phononic in-

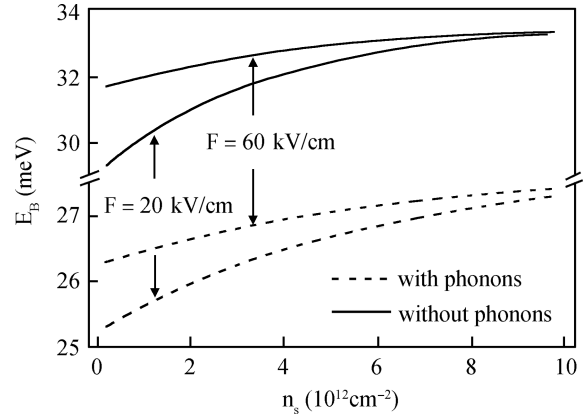


Fig. 7. Stark energy shift of polarons as a function of hydrostatic pressure for different impurity positions under an electric field $F = 20$ kV/cm.

fluence have an opposite effect compared with F to influence E_B with increasing z_0 since one effect of P is to increase the interface potential (increasing the barrier height) and the effect of the phonon is to weaken the Coulomb attraction.

The curves in Fig. 7 show how E_B as a function of areal electronic density n_s varies with electric field F for $z_0 = 4$ nm. One can see that the effect of phonons decreases the binding energies. Considering the phonon effect, when $n_s = 0.2 \times 10^{12}$ cm^{-2} , E_B decreases by 4.023 and 5.37 meV with percentages of 13.72% and 16.96% for $F = 20$ kV/cm, 60 kV/cm, respectively. When the electric field increases, the phonon influence becomes even more important. F and n_s are also helpful to increase the binding energy of an impurity. F enhances the Coulombic attraction between the electron and the impurity as $\bar{z} > z_0$. Moreover, n_s strengthens the band bending and the 2D character of the impurity state. The superposition of the two effects results in E_B increasing obviously and nonlinearly with n_s . However, phonons play a role in screening, which weakens the Coulombic interaction to influence the binding energy. Also, the influence from n_s on E_B becomes less and less with increasing F because the interface potential and phonons have a strong repulsion to restrict the increase of E_B for larger F and n_s .

5. Conclusion

A modified LLP variational method has been developed to calculate the binding energies of bound polarons in wurtzite nitride heterojunctions of $\text{GaN}/\text{Al}_x\text{Ga}_{1-x}\text{N}$ with free strain under hydrostatic pressure and the quantum confined Stark effect due to an external electric field. A simplified coherent potential approximation is extended to calculate the band-gap and high frequency dielectric constant for ternary mixed crystals. It is found that the binding energy shows a red shift or a blue shift with different impurity positions, and the influence from the HS and the IF optical phonons decreases dramatically the binding energies of bound polarons. The result shows that the binding energies increase nearly linearly with pressure under the modification of strain, whereas they increase nonlinearly with areal electronic density. The contributions from the LO-like phonon mode and one branch of IF phonon modes with a higher frequency are comparably important whereas the con-

tribution from TO-like and another branch of IF phonon modes with a lower frequency is small and can be neglected.

References

- [1] Jogai B. Effect of in-plane biaxial strains on the band structure of wurtzite GaN. *Phys Rev B*, 1998, 57: 2382
- [2] Shi J J. Interface optical-phonon modes and electron-interface-phonon interactions in wurtzite GaN/AlN quantum wells. *Phys Rev B*, 2003, 68: 165335
- [3] Pokatilov E P, Nika D L, Fomin V M, et al. Excitons in wurtzite AlGaIn/GaN quantum-well heterostructures. *Phys Rev B*, 2008, 77: 125328
- [4] Perlin P, Gorczyca I, Suski T, et al. Influence of pressure on the optical properties of $\text{In}_x\text{Ga}_{1-x}\text{N}$ epilayers and quantum structures. *Phys Rev B*, 2001, 64: 115319
- [5] Vaschenko G, Patel D, Menoni C S, et al. Significant strain dependence of piezoelectric constants in InGaIn/GaN quantum well. *Phys Rev B*, 2001, 64: 241308
- [6] Lepkowski S P, Majewski J A. Effect of electromechanical coupling on the pressure coefficient of light emission in group-III nitride quantum wells and superlattices. *Phys Rev B*, 2006, 74: 035336
- [7] Goñi A R, Siegle H, Syassen K, et al. Effect of pressure on optical phonon modes and transverse effective charges in GaN and AlN. *Phys Rev B*, 2001, 64: 035205
- [8] Ha S H, Ban S L. Binding energies of excitons in a strained wurtzite GaN/AlGaIn quantum well influenced by screening and hydrostatic pressure. *J Phys: Condensed Matter*, 2008, 20: 085218
- [9] Zhang M, Ban S L. Magnetic field influence on bound polarons in semiconductor GaAs/ $\text{Al}_x\text{Ga}_{1-x}\text{As}$ heterojunctions. *Chinese Journal of Semiconductors*, 2004, 25: 1618
- [10] Lee B C, Kim K W, Strosio M A, et al. Optical-phonon confinement and scattering in wurtzite heterostructures. *Phys Rev B*, 1998, 58: 4860
- [11] Shi J J, Chu X L, Goldys E M. Propagating optical-phonon modes and their electron-phonon interactions in wurtzite GaN/ $\text{Al}_x\text{Ga}_{1-x}\text{N}$ quantum wells. *Phys Rev B*, 2004, 70: 115318
- [12] Lü J T, Cao J C. Confined optical phonon modes and electron-phonon interactions in wurtzite GaN/ZnO quantum wells. *Phys Rev B*, 2005, 71: 155304
- [13] Ban S L, Hasbun J E. Donor level in a quasi-two dimensional heterojunction system. *Solid State Commun*, 1999, 109: 93
- [14] Wagner J M, Bechstedt F. Properties of strained wurtzite GaN and AlN: *ab initio* studies. *Phys Rev B*, 2002, 66: 115202
- [15] Lepkowski S P. Nonlinear elasticity effect in group III-nitride quantum heterostructures: *ab initio* calculations. *Phys Rev B*, 2007, 75: 195303
- [16] Perlin P, Mattos L, Shapiro N A, et al. Reduction of the energy gap pressure coefficient of GaN due to the constraining pressure of the sapphire substrate. *J Appl Phys*, 1999, 85: 2385
- [17] Shan W, Hauenstein R J, Fischer A J, et al. Strain effects on excitonic transitions in GaN: deformation potentials. *Phys Rev B*, 1996, 54: 13460
- [18] Christensen N E, Gorczyca I. Optical and structural properties of III-V nitride under pressure. *Phys Rev B*, 1994, 50: 4397
- [19] Ban S L, Hasbun J E. Interface polarons in a realistic heterojunction potential. *Eur Phys J B*, 1999, 8: 453
- [20] Nardelli M B, Rapcewicz K, Bernholc J. Strain effects on the interface properties of nitride semiconductors. *Phys Rev B*, 1997, 55: R7323
- [21] Ting D Z Y, Chang Y C. Γ -X mixing in GaAs/ $\text{Al}_x\text{Ga}_{1-x}\text{As}$ and $\text{Al}_x\text{Ga}_{1-x}\text{As}/\text{AlAs}$ superlattices. *Phys Rev B*, 1987, 36: 4359
- [22] Goñi A R, Syassen K, Cardona M. Effect of pressure on the refractive index of Ge and GaAs. *Phys Rev B*, 1990, 41: 10104
- [23] Vurgaftman I, Meyer J R, Ram-Mohan L R. Band parameters for III-V compound semiconductors and their alloys. *J Appl Phys*, 2001, 89: 5815
- [24] Wagner J M, Bechstedt F. Pressure dependence of the dielectric and lattice-dynamical properties of GaN and AlN. *Phys Rev B*, 2000, 62: 4526
- [25] Zhang M, Ban S L. Pressure influence on the Stark effect of impurity states in a strained wurtzite GaN/ $\text{Al}_x\text{Ga}_{1-x}\text{N}$ heterojunction. *Chinese Physics B*, 2009, 18: 4449